

SEDIMENT ENTRAINMENT DUE TO SHEAR FLOW

See Whan Kang

Korea Ocean Research and Development Institute KAIST, Seoul 135, Korea

ABSTRACT

A series of experiments was performed to increase and make our quantitative understanding of the entrainment and settling processes of fine-grained sediments, which are of critical importance to construct a predictive model of sediment transport. Two different sediments from Lake Michigan were analyzed. The entrainment experiments were performed in an annular flume. A rotating top produced a turbulent flow which in turn exerted a shear stress at the sediment-water interface. Large variations in settling velocities occurred and are shown to be dependent on the sediment concentration and the presence of clay minerals. The parameters on which entrainment strongly depends were identified to be the shear stress, water content (time after deposition), and the type of sediment (grain size and mineralogy).

INTRODUCTION

Sediments are significant contaminants since they increase the turbidity of the water and, when heavy sedimentation occurs, may require that large amounts of dredging be done. In addition, most importantly in the present context of water pollution, fine-grained (clays or silts) sediments readily absorb many other contaminants such as phosphates, heavy metals, and toxic hydrocarbons. Hence, if we understand the transport of sediments, we can then more readily understand the transport and fate of other contaminants. This is the justification for the present study.

The primary sources of suspended sediments in a coastal water are in general river inflow and shore erosion while the primary sinks are the deposition and ultimate consolidation of sediments into the permanent sedimentary bottom of the offshore. The process of the transport of sediments from the primary sources to ultimate sinks occurs by frequent cycles of resuspension, transport, and deposition. Because

of this, in shallow waters, the major immediate source of sediments in the water column is resuspension from the bottom, the sediment-water interface, rather than river inflows or shore erosion (Kang et al, 1982). The resuspended sediments are then transported both vertically and horizontally by currents, turbulent diffusion, and settling.

The basic equation describing sediment transport is the mass balance, or conservation, equation:

$$\begin{aligned} \frac{\partial C}{\partial t} + \frac{\partial(uC)}{\partial x} + \frac{\partial(wC)}{\partial y} + \frac{\partial[(w+w_s)C]}{\partial z} \\ = -\frac{\partial}{\partial x} D_H \frac{\partial C}{\partial x} + \frac{\partial}{\partial y} D_H \frac{\partial C}{\partial y} \\ + \frac{\partial}{\partial z} D_V \frac{\partial C}{\partial z} + S \end{aligned} \quad (1)$$

where C is the concentration of the sediments, t is time, u, v , and w are fluid velocities in the x, y, z directions respectively (where z is vertical), w_s is the settling speed of the sediments, D_H is the horizontal eddy diffusivity, D_V is the vertical eddy diffusivity, and S is a source term.

In order to obtain solutions of equation (1) in addition to other parameters, the net flux of sediment at the air-water interface (generally

assumed to be negligible) and at the sediment-water interface must be determined (Sheng and Lick, 1979). This latter flux, denoted by q_s , can be written as the difference between the entrainment rate E and the deposition rate D , or

$$q_s = E - D \quad (2)$$

Here the assumption has been made that entrainment and deposition are independent processes, *i.e.*, E is the sediment flux when no suspended sediment and therefore no deposition is present and D is the sediment flux in the absence of entrainment (Fukuda and Lick, 1980).

Deposition may be due to several different mechanisms, *e.g.*, settling of particles, kinetic impaction and mechanical capture, electrostatic effects, and chemical reaction. The simplest plausible hypothesis for the deposition rate is that it is proportional to the local concentration at the sediment-water interface (Monin, 1959; Calder, 1961; Monin and Yaglom, 1973), and therefore

$$q_s = E - \beta C \quad (3)$$

where β is the coefficient of proportionality, is known as the reflectivity parameter, and has the units of velocity. In steady state, $q_s = 0$, and a steady-state concentration C_s can be defined by $E - \beta C_s = 0$. As in the case of the mass balance equation, the hypothesis that $D = \beta C$ is probably strictly valid only for sediments of uniform particle size (Massion et al, 1983) and is only an approximation for naturally occurring sediments which have effective particle sizes varying over several orders of magnitude.

The processes that govern entrainment and deposition are not well understood especially for fine-grained sediments. In the present study, the experiments were conducted in an annular flume (Figure 1). We have investigated these processes, mainly emphasizing settling speed and entrainment, for two sediments from Lake Michigan.

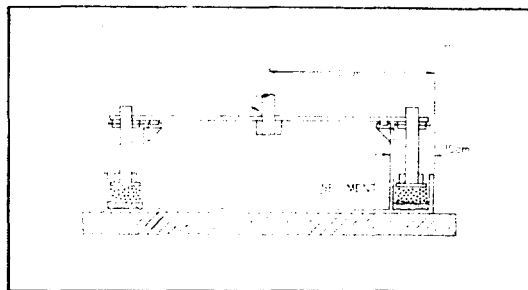


Fig. 1. Schematic diagram of annular flume.

SETTLING VELOCITIES AND SEDIMENT PROPERTIES

The settling speed-frequency distributions for the two sediments from Lake Michigan have been obtained in a settling tube by the pipette method. The results are shown in Figure 2 (for sediment #7) and Figure 3 (for sediment #14). Percent of sediment having settling speeds within various intervals for tap water, presumably closely corresponds to lake water.

From the figures, it can be seen that the settling velocities range over more than four orders of magnitude. Hence, the effective sizes of particles are also distributed over several orders of magnitude. In tap water, flocculation occurs and the settling velocity depends quite strongly on the sediment concentration (Migniot, 1968). The median settling velocities for the concentrations of sediment #7, 0.5, 2.1, 5.8, and 13.7 g/l are respectively 1.3×10^{-3} , 2.6×10^{-2} , 5.7×10^{-2} , and 7.5×10^{-2} cm/sec. Sediment #14 also shows similar changes in settling velocities, 1.9×10^{-2} , 4.1×10^{-2} , 7.7×10^{-2} , 1.6×10^{-1} , and 2.5×10^{-1} cm/sec for the concentrations of 0.9, 1.5, 4.4, 10.6, and 22.2 g/l respectively.

For flocculation to occur, particle must collide and, after collision, must cohere. Cohesion of particles depends generally on the mineralogy of the particles, the particle sizes, and on the

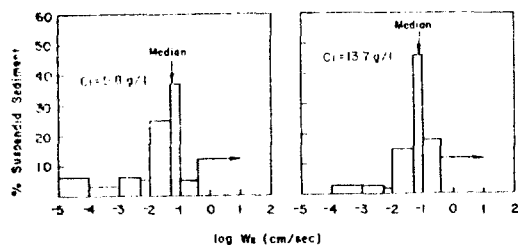
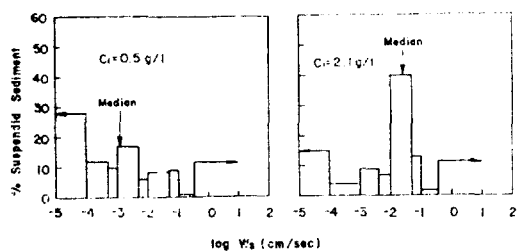


Fig. 2. Settling velocity distributions for sediment #7 in tap water. Percent by mass of sediments as a function of settling velocity.

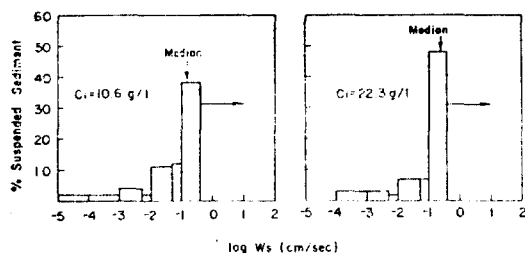
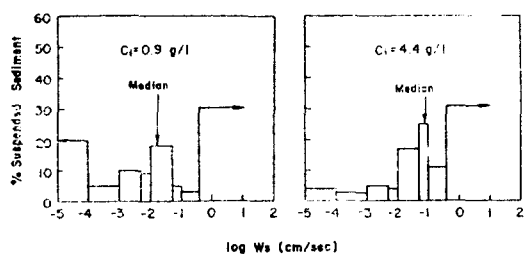


Fig. 3. Settling velocity distributions for sediment #14 in tap water. Percent by mass of sediments as a function of settling velocity.

quantity and type of cations present in solution. Table 1 shows the mineral composition of the two samples as determined by X-ray diffraction method (Carroll, 1970). Also shown are the results for sediment #4 from the Lake Erie (Lee, et al, 1981). It can be seen that sediments

Table 1. Mineral Composition of the Sediments(%).

Sediment Source	Lake Michigan sediment #7	Lake Michigan sediment #14	Lake Erie sediment #4
Clay	13	13	40
Quartz	44	44	39
Dolomite	38	33	7
Alkali Feldspar	5	6	12
Calcite	0	4	2

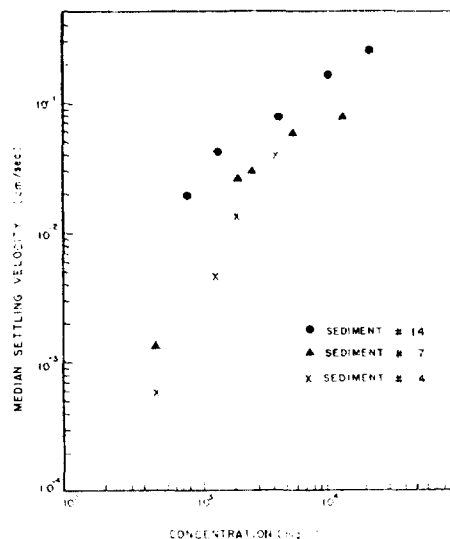


Fig. 4. Variations of the median settling velocities for various initial concentrations.

#7 and #14 are fairly similar in mineralogy, i.e., they are high in quartz and dolomite, and low in clay (13%) while sediment #4 is high in both quartz and clay (40%). This difference is also evident in the settling velocities for the concentrations. The median settling velocity of sediment #4 increases approximately two orders of magnitude as the concentration increases from 0.5 g/l to 4 g/l (Figure 4).

EXPERIMENT

Channel Flow and Shear Stress

The experiments were performed in an annular channel, 15 cm wide and 2 m in diameter (Figure 1). Five cm water column was used for all the experiments. A rotating top produced a turbulent

flow which in turn exerted a shear stress on the sediment-water interface.

To measure the velocity profiles in the turbulent boundary layer flow, laser Doppler anemometer (DISA 55L 90a) was used.

The velocity profiles were taken at two radial positions, $R'=0.2$ and 0.8 . Here, R' is defined as $R' = (r - r_i) / (r_0 - r_i)$, where r is the radial position, r_i and r_0 are the radial positions of the inner and outer side-walls, respectively. The law of the wall was used to calculate bottom shear stress from the mean velocity profiles and is given by

$$U^+ = A \ln Z^+ + D \text{ for } Z^+ > 30 \sim 40 \quad (4)$$

where $U^+ = U/u^*$, $Z^+ = zu^*/\nu$, $\tau_w = \rho u^{*2}$ where u^* is the friction velocity, z is the distance above the wall, ν is the kinematic viscosity, ρ is the fluid density, τ_w is the wall shear stress, and A and D are constants. Here, the bottom surface was assumed to be hydrodynamically smooth.

In the presence of rough elements on the bottom surface, the boundary layer flows are altered because of turbulent wakes and vorticities. The roughness Reynolds number is defined as

$$R_K = K_s u^*/\nu \quad (5)$$

where K_s is an rms roughness height. If R_K is less than 5, the sediment-water interface can be considered a smooth surface (Tennekes and Lumley, 1972). The R_K values for all sediments and flow conditions used in this study were less than 2. The use of equation (4) is justified.

To determine the frictional velocity, u^* and then the shear stress, τ_w , equation (4) was iterated for each velocity profile. The frictional velocities in the logarithmic region were averaged to give the shear stress for that profile. In Figure 5 the velocity data in the turbulent boundary layer flow are plotted in the nondimensional coordinates, U^+ and Z^+ . The line over the logarithmic region was calculated by $A=2.54$ and $D=5.56$

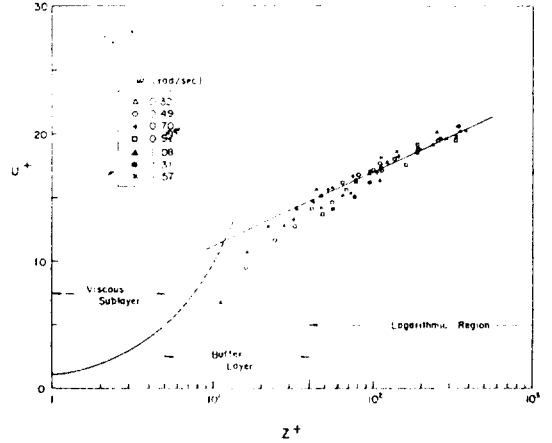


Fig. 5. Velocity profiles at $R'=0.8$ in the non-dimensional wall coordinates.

for the smooth plate (Schlichting, 1979). The mean velocity increases with distance from the inner wall of the channel causing the shear stress to vary radially across the channel. Hence, at a particular rotation rate the shear stresses were then averaged to give the average bottom shear stress (Figure 6).

Entrainment

Entrainment experiments were conducted as follows. The sediments in the flume were first thoroughly mixed with the overlying water and then allowed to settle for the desired time periods. At this time, the water was at rest and

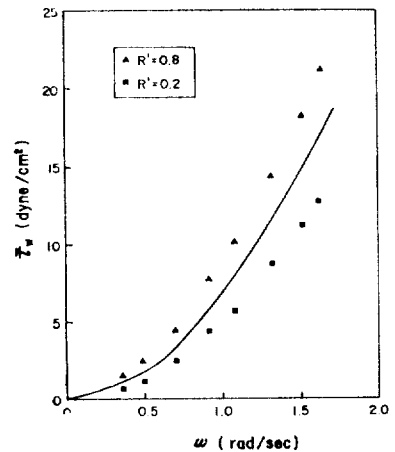


Fig. 6. Averaged bottom shear stress with rotating rate.

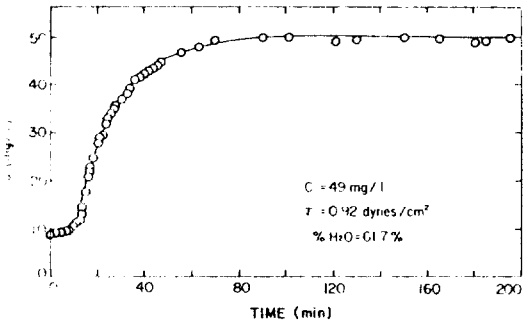


Fig. 7. Sediment concentration as a function of time during a typical entrainment experiment.

the sediment concentration in the overlying water was approximately zero. The lid of the flume was then rotated at a constant speed corresponding to the desired stress. Because of this, the sediments were entrained and the sediment concentration in the overlying water increased rapidly at first and then more slowly until a steady state was reached where the entrainment is balanced by deposition. A typical concentration versus time plot is shown in Figure 7. The steady-state concentration is directly measured while the entrainment rate can be deduced from the initial slope of the curve.

Results of these experiments for Sediment #7 and Sediment #14 are shown in Figures 8, 9, 10, and 11. Figure 8 and 9 show steady-state concentrations as a function of shear stress with water content (or time after deposition) as a parameter. The range of water content corresponds to deposition times of one to six days, approximately to the time between strong wind events on the Great Lakes. The entrainment rates and reflectivity parameters for two sediments are compared in Figures 10 and 11.

It can be seen that both C_s and E are strong functions of shear stress and water content. Typically, C_s and E change very rapidly (on a logarithmic scale) at low stresses, *i.e.*, $\tau_w \leq 4 \sim 5$ dynes/cm² and more slowly as the stress increases. As length of compaction time increases,

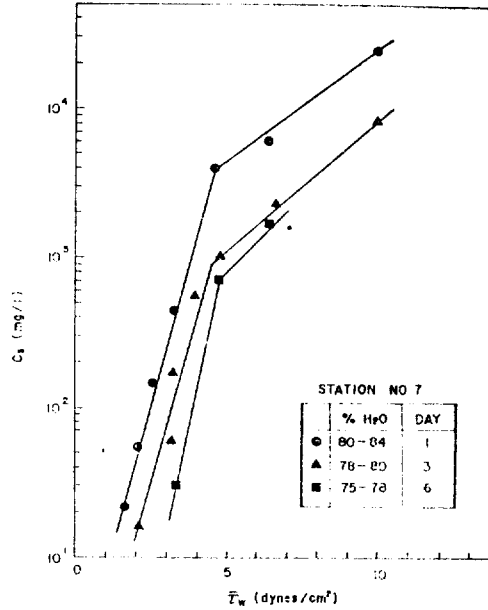


Fig. 8. Steady-state concentration as a function of shear stress with water content (time after deposition) as a parameter. Sediment #7.

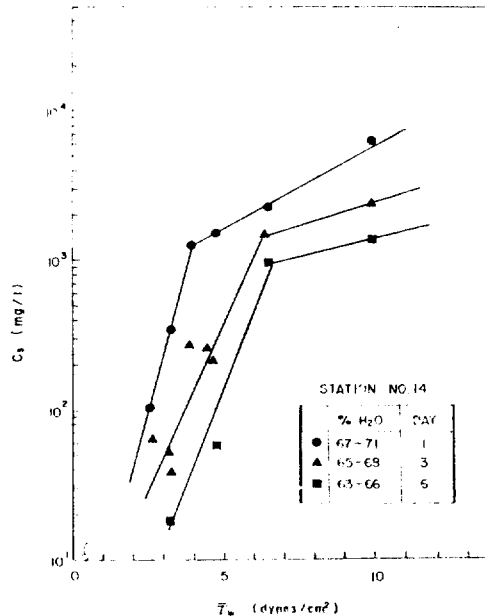


Fig. 9. Steady-state concentration as a function of shear stress with water content (time after deposition) as a parameter. Sediment #14.

C_s and E decrease. Over these changes of water content, C_s and E both change by more than an order of magnitude. It appears that β changes

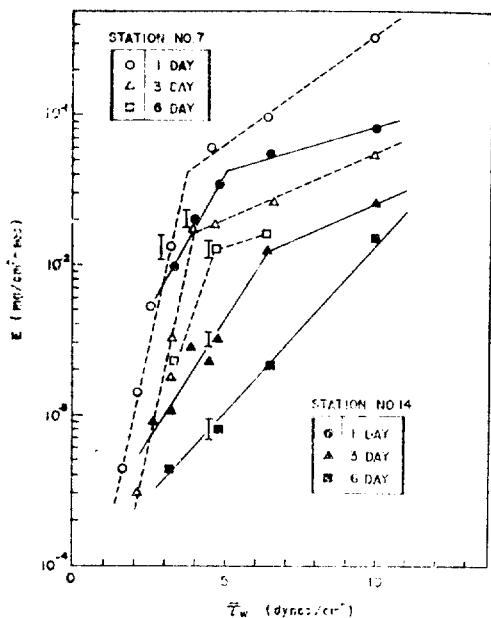


Fig. 10. Entrainment rate as a function of shear stress with water content as a parameter, less compared to the variations in C_s and E and decreases as τ_w increases.

Sediment #7 was rather easily erodible than sediment #14. As shown in Figure 2 and 3, sediment #14 has larger average grain size, especially with large fraction of coarse particles. This can be explained that for a particular shear stress, the coarser particles retained on

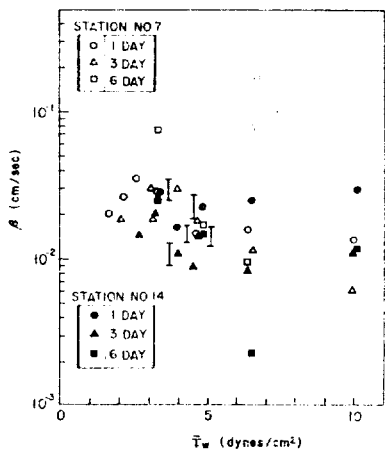


Fig. 11. Reflectivity parameter as a function of shear stress with water content as a parameter.

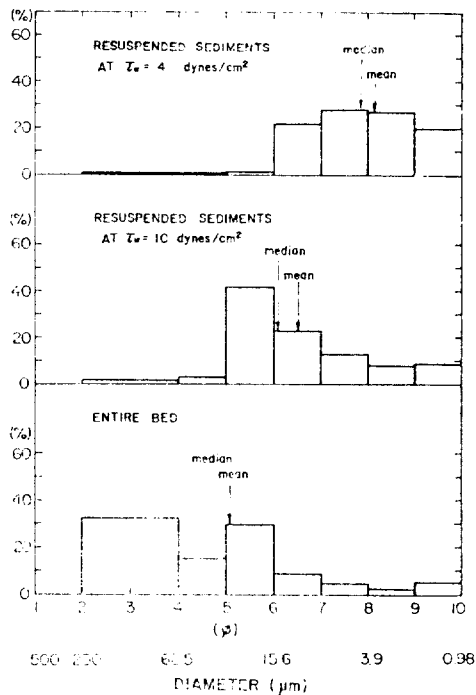


Fig. 12. Particle size distribution for sediments resuspended at shear stresses (dynes/cm²) of 4, 10, and infinity. Sediment #14.

the bed protect the finer particles beneath from entrainment, thus armoring the bed.

This entrainment process was studied in more detail by analyzing the particle size of the resuspended sediment. In Figure 12 are shown the effective particle size distributions of sediments for shear stresses of 4 and 10 dynes/cm² and also for the well mixed sediments corresponding to complete entrainment of infinite shear stress. It can be seen that fine particles are entrained at the lower stress and coarser particles are entrained as the stress increases.

SUMMARY AND CONCLUSIONS

A series of experiments has been performed to increase and make quantitative our understanding of entrainment and settling processes of fine-grained sediments. These quantities must be known or determined to predict sediment transport (as suspended load) in a coastal water.

In the present study, two different sediments from Lake Michigan were analyzed. It has been shown that large variations in settling speed are strongly depending on the sediment concentration, grain size, and mineralogy. The steady-state concentration and entrainment rate increase very rapidly (on a logarithmic scale) at low stress and more slowly at high stress. Both C_s and E decrease with increasing compaction time and also depend on the type of sediment. It has been indicated that at the lower stress fine particles are entrained first, and then coarser particles are entrained as the stress increases.

Before a quantitative, predictive model of sediment transport is constructed, much more study is needed. The present studies have only examined the surficial sediment layer and not the entrainment of the lower, more compacted sediments. Effects of benthic organisms have not been considered. Only entrainment due to a steady flow has been considered. In a coastal area, especially in shallow waters where most entrainment occurs, the main cause of entrainment is oscillatory wave action, a mechanism which must be considered in future work.

ACKNOWLEDGMENTS

This research was performed while the author was in the University of California-Santa Barbara. The author wishes to thank Mr. C.B. Lee for drawing figures and Ms. N.S. Lee for typing the manuscript.

REFERENCES

- Calder, K.L., 1961. Atmospheric Diffusion of particulate matter considered as a boundary value problem, *J. of Meteorology*, 18(3):413-416
- Carroll, D., 1970. Clay minerals: A guide to their X-ray identification, The Geological Society of America, special paper 126
- Fukuda, M.K. and W. Lick, 1980. The entrainment of cohesive sediments in fresh water, *J. Geophysical Research*, 85:2813-2624
- Kang, S.W., Sheng, Y.P., and W. Lick, 1982. Wave action and bottom shear stresses in Lake Erie, *J. Great Lakes Res.* 8:482-494.
- Lee, D.Y., W. Lick, and S.W. Kang, 1981. The entrainment and deposition of fine-grained sediments in Lake Erie, *J. Great Lakes Res.* 7:224-33
- Massion, G., S.W. Kang and W. Lick, 1983. Entrainment and deposition of uniform-size finegrained sediment. to be published
- Migniot, C., 1968. Étude des propriétés physique de différents sédiments très fins et de leur comportement sus des actions hydrodynamiques, *La Houille Blanche*, 23(7):591-620.
- Monin A.S., 1959. On the boundary condition on the earth's surface for diffusing pollution, *Advances in Geophysics*, 6, Academic Press, New York.
- Monin, A.S. and A.M. Yaglom, 1973. *Statistical fluid mechanics*, 1, The MIT Press, Cambridge, MA.
- Schlichting, H., 1979. *Boundary layer theory*, 7th ed., McGraw-Hill, New York
- Sheng, Y.P. and W. Lick, 1979. The transport and resuspension of sediments in a shallow Lake, *J. Geophysical Research*, 84:1809-1826
- Tennekes, H. and J.L. Lumley, 1972. *A first course in turbulence*, The MIT Press, Cambridge, MA.

剪斷流에 의한 堆積物 浮上

姜 始 桓

한국 과학 기술원 해양연구소

要 約

堆積物 流動의 再現과 豫測을 爲한 數值模型의 開發에는 堆積物의 浮上機作과 沈澱過程의 究明이 先決要件이 된다.

따라서 이의 究明을 爲한 一連의 水理實驗이 企圖되었다.

研究結果, 堆積物의 浮上은 전단응력과 퇴적물에 함유된 수분량 및 堆積物의 구성종류에 따라 좌우되고 있음이 밝혀졌으며, 침전은 퇴적물의 농도와 점토광물질의 함유량에 따라 크게 변하고 있음이 밝혀졌다.